**Proceedings of OMAE'02**
**21st International Conference on Offshore Mechanics and Arctic Engineering**
**June 23-28, 2002,Oslo, Norway**

**OMAE2002-28083**

# ELASTOPLASTIC ANALYSIS OF THE RESIDUAL STRESS IN CHAIN LINKS

**Pedro M. Calas Lopes Pacheco**
CEFET/RJ
Dept. of Mech. Engineering
20.271-110 - Rio de Janeiro, RJ
Brazil
Tel/Fax: 55-21-2569-4495
e-mail: calas@cefet-rj.br

**Paulo Pedro Kenedi**
CEFET/RJ
Dept. of Mech. Engineering
20.271-110 - Rio de Janeiro, RJ
Brazil
Tel/Fax: 55-21-2569-4495
e-mail: pkenedi@cefet-rj.br

**Jorge Carlos Ferreira Jorge**
CEFET/RJ
Dept. of Mech. Engineering
20.271-110 – Rio de Janeiro, RJ
Brazil
Tel/Fax: 55-21-2569-4495
e-mail: jorge@cefet-rj.br

## ABSTRACT

Mooring lines of offshore oil exploitation platforms consist of long lengths of steel chain links, wire ropes and other accessories. Usually, these lines are designed for an operational life of about 20 years and periodic inspections are mandatory for monitoring the structural integrity of these components. The failure of a single element in a mooring line can cause incalculable environmental damage and severe economic losses. The ocean adverse environment loading produced by the combination of the wind, waves and currents leads to a complex alternate loading that can promote fatigue and crack propagation. Residual stress plays a preponderant part in the structural integrity of a mechanical component subjected to such loading. Offshore mooring line components as chain links enter in operation with a residual stress field created by the proof test dictated by offshore standards. However, the traditional design of such mechanical components does not consider the presence of residual stress. This study concerns about predict the residual stress field present in stud and studless chain links prior to operation to compare the fatigue life predicted by the traditional design methodology with the one predicted considering the residual stresses states present before operation. Numeric simulations with an elastoplastic finite element model are used to estimate the residual stress along the chain link that are present after the proof test and before operation. The results indicate that the presence of residual stresses modify significantly the fatigue life of the component.

## INTRODUCTION

The continuous expansion of deepwater activities has resulted in increasing attention on the design of mooring systems [1-3]. The failure of a single element in a mooring line of an offshore oil exploitation platform can produce incalculable environment damage and heavy economical loses. Indeed, traditional design and inspection methodologies are very conservative [4-6]. To permit the use of simple design methodologies, such effects as the presence of residual stress fields promoted by fabrication processes are not considered in the analysis. Meanwhile, it is well know that residual stress plays a preponderant part in the structural integrity of a mechanical component, especially in its fatigue life [7-9]. Therefore, a detailed knowledge of the residual stress field is required for an accurate assessment of a mechanical component fatigue lifetime. The ocean adverse environment loading produced by the combination of the wind, waves and currents leads to a complex alternate loading that can promote fatigue and crack propagation. As fatigue cracks are normally initiated by a tensile stress field, the presence of tensile residual stresses can be especially dangerous. In the presence of tensile stresses promoted by the normal loading conditions, both stresses are added resulting in much higher tensile stress levels than the predicted ones by the design process. On the other way, a compressive residual stress can be beneficial if, during operation, it is subtracted from a tensile one generated by the normal loading.

 Copyright © 2002 by ASME

Downloaded From: https://proceedings.asmedigitalcollection.asme.org on 06/27/2019 Terms of Use: http://www.asme.org/about-asme/terms-of-use

The present contribution regards on study the influence of residual stress fields on the structural integrity of offshore stud and studless chain links. Before operation, every chain link must be submitted to a mandatory proof test where loads as high as three times the operational load are applied to the mechanical component, resulting in high levels of residual stresses. Numeric simulations with an elastoplastic finite element model are used to estimate the residual stress field along the chain link that are present after the proof test and, therefore, before operation. Both constitutive and geometric nonlinearities are considered. A simplified analysis of the effect of the residual stresses in the fatigue life of a 92 mm chain link (stud and studless) based on *S-N* curve is presented. The analysis shows that the residual stress plays a preponderant part in the structural integrity of chain links.

## MODEL

A tri-dimensional finite element elastoplastic model was developed to study the residual stresses in stud and studless chain links. In order to simplify the analysis, three planes of symmetry were considered, as shown in Figure 1. Numerical simulations were performed with the commercial finite element code ANSYS, Release 5.7. The elements SOLID95 (20 nodes brick structural solid - 3 degree of freedom per node), and SOLID92, (10 node tetrahedral structural solid - 3 degree of freedom per node), were used [10]. The final meshes were defined after a convergence study. A pressure distribution applied at the contact area between the chain and the other mooring elements was adopted to simulate the loading condition. The pressure distribution was assumed to be equivalent to the resultant load in the region, and varies linearly from a maximum value to zero at the border of the contact area. An angle of 35 degrees with the axial direction was selected to represent the contact area between the chain and the mooring line. As the model does not capture the contact phenomenon that occurs between two chain links the results near this region are not representative. In the proposed model symmetry boundary conditions were applied to the three planes of symmetry. The geometry of stud and studless chain links was designed in accordance with ISO 1704 recommendation [11]. For a circular section with diameter *d*, the length is equal to 6*d* for both links and the maximum width is 3.35*d*. In this study the maximum width value was adopted.

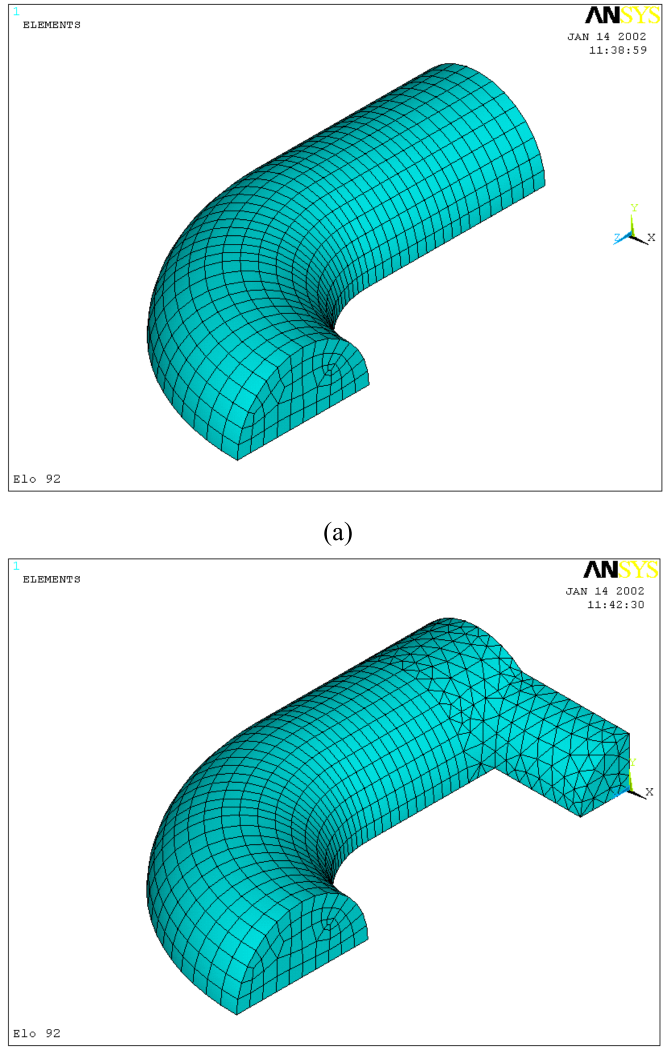


**Figure 1 – Finite element model. (a) Studless and (b) stud chain link meshes.**

## NUMERICAL SIMULATIONS

Numerical simulations were developed to estimate the residual stress distribution present in the stud and studless chain links before operation. This residual stress field is promoted by the mandatory proof test. The fabrication process involves the bending and welding of a steel bar and is executed at high temperatures. It is assumed that there is no residual stress field present prior to the proof test.

The condition prior to operation is achieved by first applying and then removing the recommended proof load, considering an initial material state prior to the proof load. For the simulations presented the following properties were adopted to represent this prior material state: elastic modulus (E) of 207 GPa, Poisson coefficient ($\nu$) of 0.29, yield strength ($S_y$) of 600 MPa and tensile strength ($S_{ut}$) of 720 MPa and an elongation associated to the tensile strength of 12% [12]. The stresses and


Copyright © 2002 by ASME

Downloaded From: https://proceedings.asmedigitalcollection.asme.org on 06/27/2019 Terms of Use: http://www.asme.org/about-asme/terms-of-use

strains were transformed from engineering values to real values and used to represent the elastoplastic behavior of the material by a bilinear kinematic hardening material [10]. Also, a proof load of 4382 kN was adopted, according to API 2F [12] for a 92 mm diameter chain link.

The numerical results show that extensive plasticity develops in the whole component due to the initial proof load. As a consequence, high values of residual stresses (higher than the initial yield strength) are present after the load removal. Figure 2 shows the *von Mises* equivalent residual stress present after the proof load. The condition obtained after the application of the proof load is named in this work as *tested*.

It is important to mention that high residual compressive stresses are observed in regions where higher stresses develop during the initial proof load. This effect can be highly beneficial for the fatigue strength of the component as the operational load is lower than the proof load and, therefore, these regions work with a lower value of mean stress component or even with only compressive stresses. Figure 3 shows the *von Mises* equivalent stress promoted by the application of the operational load for both studless an stud chain links in a tested condition for an elastoplastic model. An operational load equal to one third the proof load is considered.

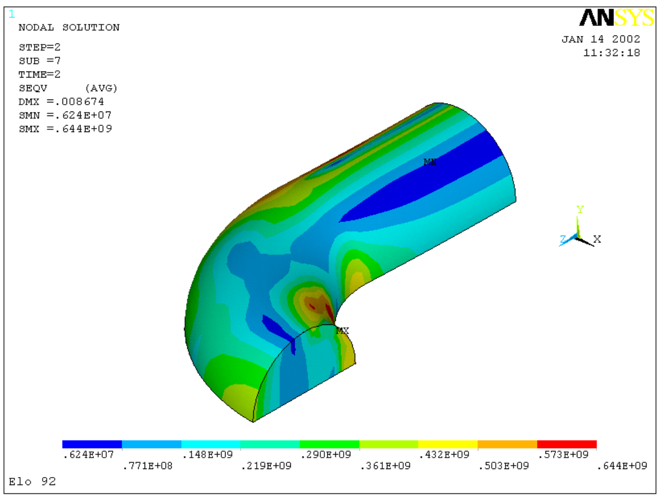


(a)

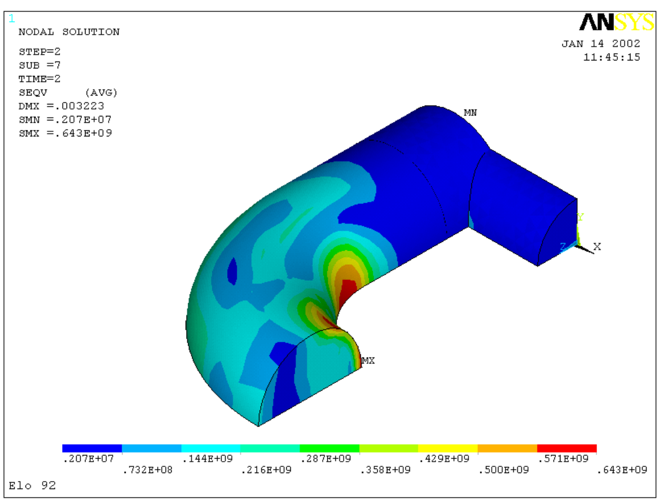


(b)

**Figure 2 – *von Mises* equivalent residual stress. (a) Studless and (b) stud chain links. Elastoplastic model.**

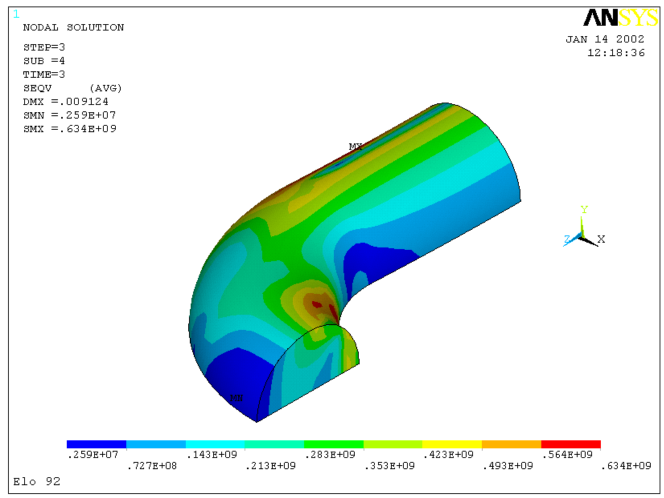


(a)

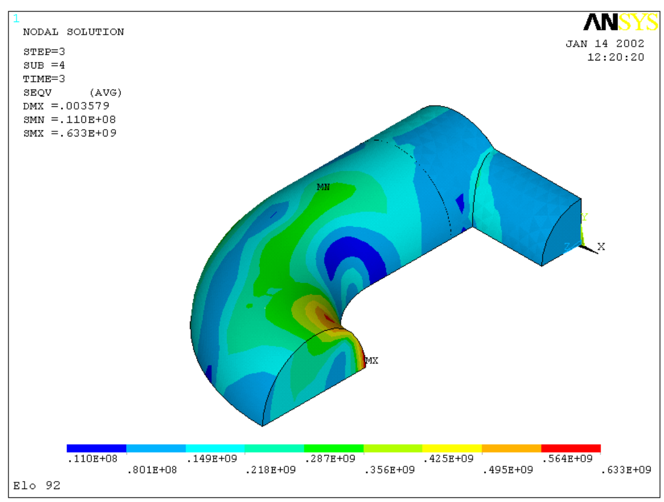


(b)

**Figure 3 – *von Mises* equivalent stress for operational loading. (a) Studless and (b) stud chain links. Elastoplastic model.**


Copyright © 2002 by ASME

Downloaded From: https://proceedings.asmedigitalcollection.asme.org on 06/27/2019 Terms of Use: http://www.asme.org/about-asme/terms-of-use

Figure 4 shows the *von Mises* equivalent stress promoted by the application of the operational load for both studless and stud chain links considering a fully elastic component. In this case, there are no prior residual stresses, and a completely different stress distribution, from the one shown in Figure 3, was obtained. These results suggest that an elastic analysis of the chain links is not sufficient to support a reliable fatigue analysis of this type of mechanical component.

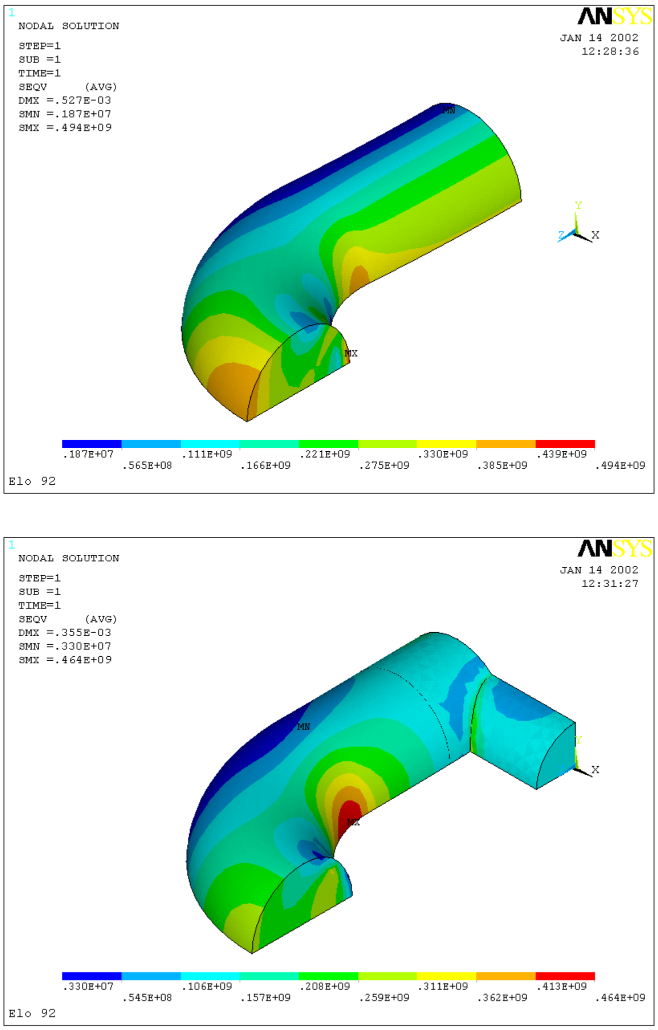


**Figure 4 – *von Mises* equivalent stress for operational loading. (a) Studless and (b) stud chain links. Elastic model.**

As expected, this behavior is also observed for the maximum principal stress ($\sigma_1$). Figures 5 and 6 show the maximum principal stress for the elastoplastic and elastic models submitted to the operational load.

The developed stresses were also accomplished in two sections (*A* and *B*) and along five longitudinal paths (*a*, *b*, *c*, *d* and *e*) shown in Figure 7. Figures 8-10 show the longitudinal stress distributions for the two sections analyzed (*A* and *B*). Figure 8 shows the residual stress distribution and Figures 9 and 10 show the stresses distribution promoted by the operational load for the elastoplastic and elastic models, respectively. Figures 11 and 12 show, respectively, the *von Mises* equivalent stress and the maximum principal stress promoted by the application of the operational load for both elastoplastic and elastic models for the five longitudinal paths (*a*, *b*, *c*, *d* and *e*). As observed in Figures 3-6, elastoplastic and elastic models furnish completely different stress distributions.

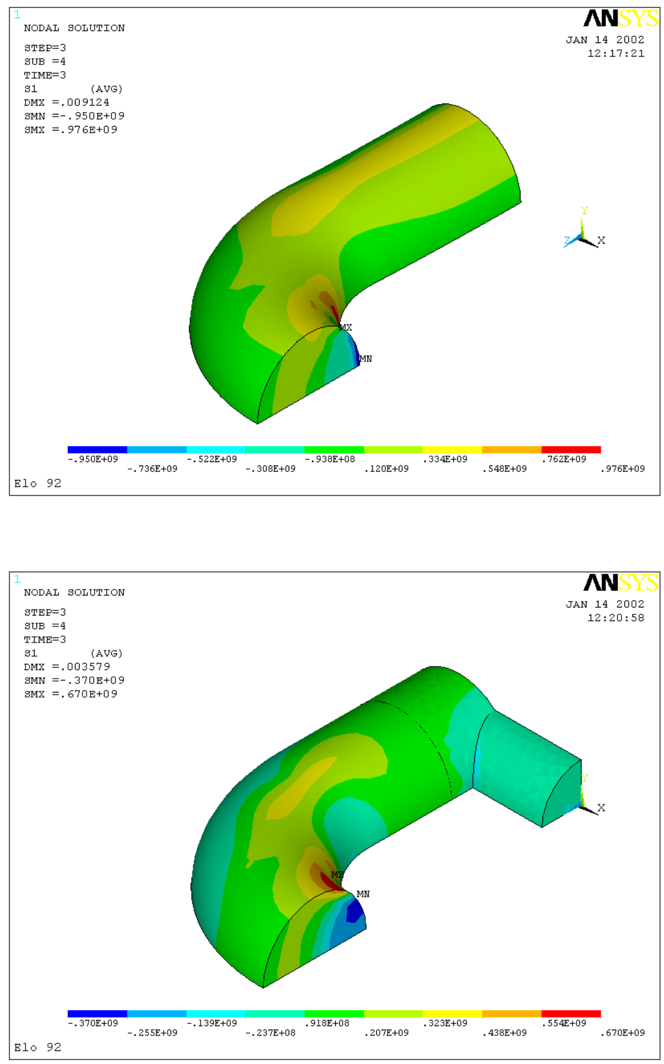


**Figure 5 – Maximum principal stress for operational loading. (a) Studless and (b) stud chain links. Elastoplastic model.**


Copyright © 2002 by ASME

Downloaded From: https://proceedings.asmedigitalcollection.asme.org on 06/27/2019 Terms of Use: http://www.asme.org/about-asme/terms-of-use

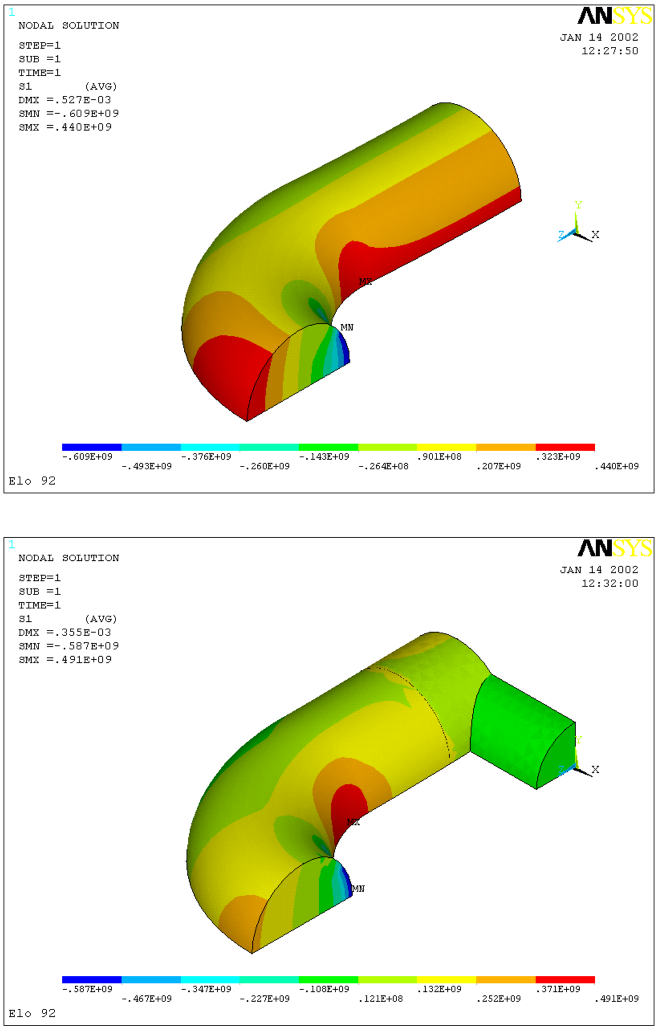


**Figure 6 – Maximum principal stress for operational loading. (a) Studless and (b) stud chain links. Elastic model.**

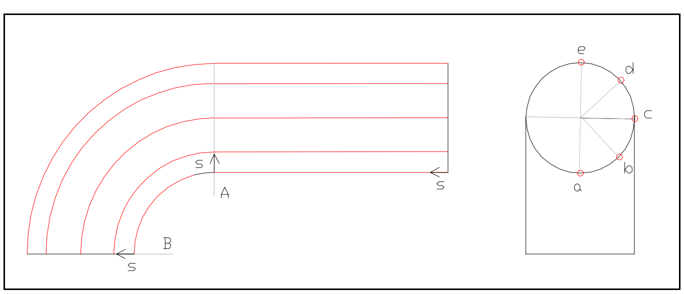


**Figure 7 –Sections (A and B) and paths (a, b, c, d, e) analyzed.**

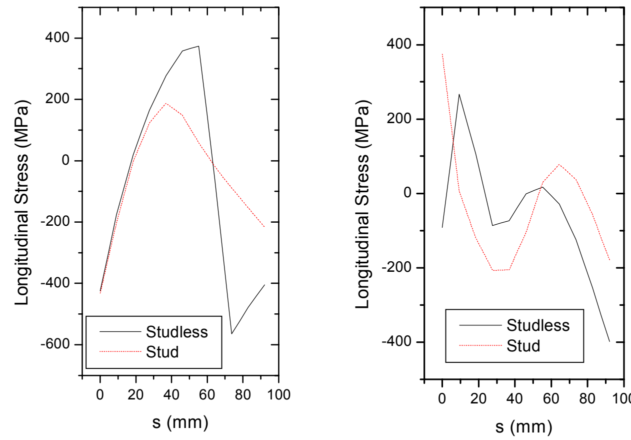


**Figure 8 – Longitudinal residual stress in sections A and B. Elastoplastic model.**

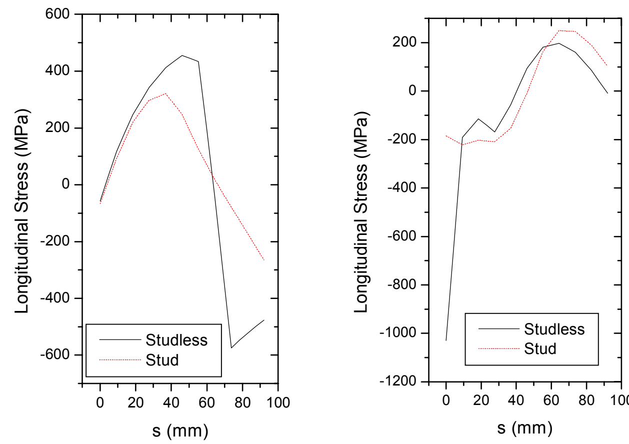


**Figure 9– Longitudinal stress in sections A and B. Operational loading. Elastoplastic model.**

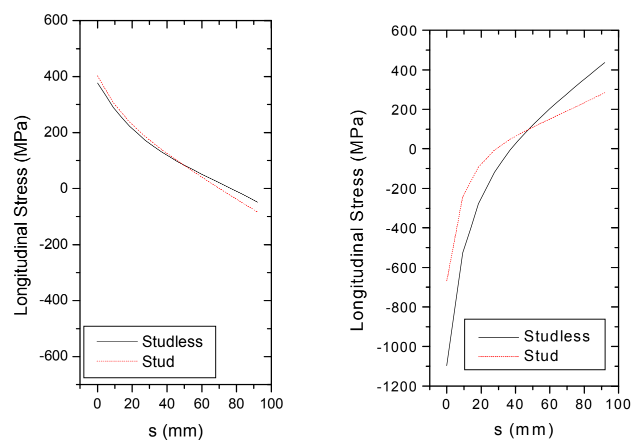


**Figure 10 – Longitudinal stress in sections A and B. Operational loading. Elastic model.**


Copyright © 2002 by ASME

Downloaded From: https://proceedings.asmedigitalcollection.asme.org on 06/27/2019 Terms of Use: http://www.asme.org/about-asme/terms-of-use

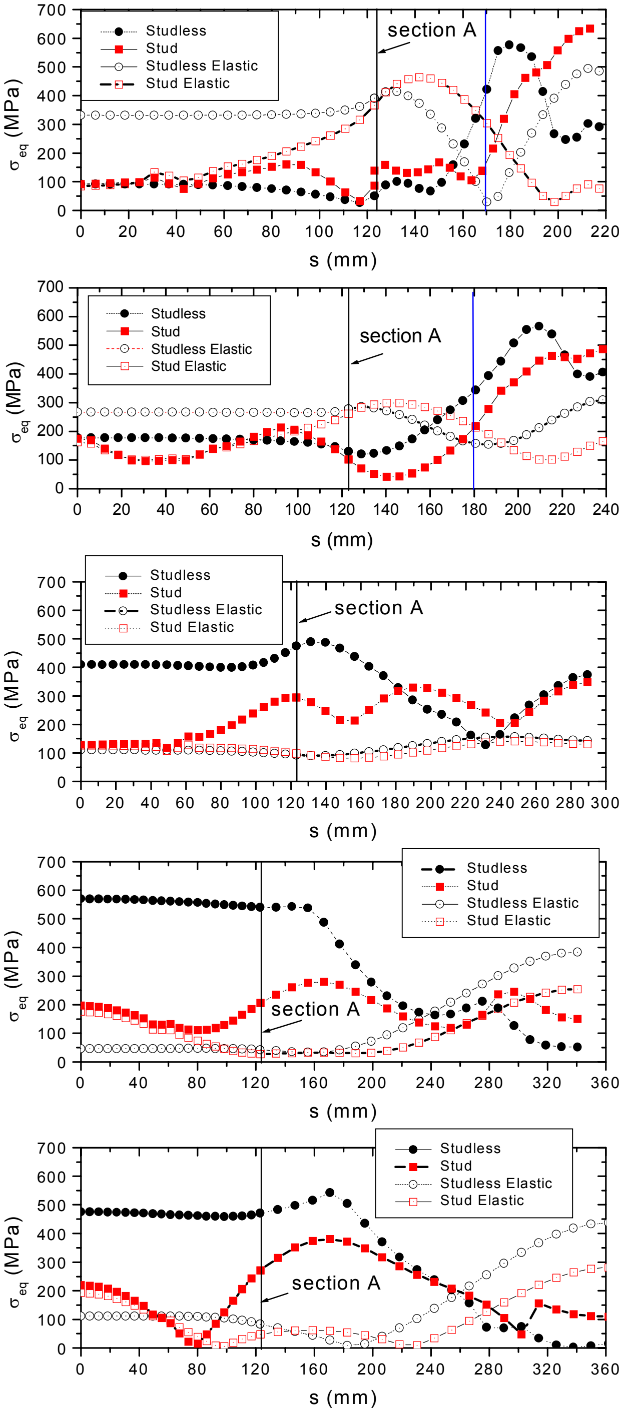


**Figure 11 – *von Mises* equivalent stress for operational load. Paths *a*, *b*, *c*, *d*, *e*.**

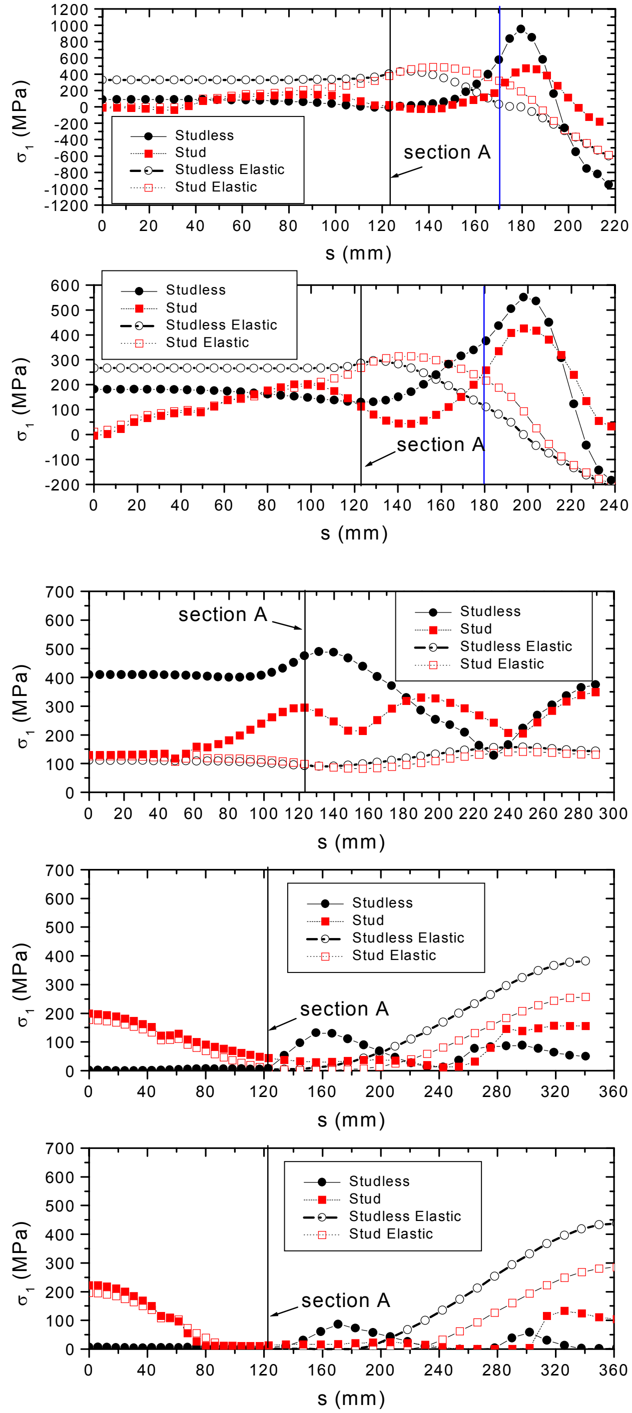


**Figure 12 – Maximum principal stress for operational load. Paths *a*, *b*, *c*, *d*, *e*.**


Copyright © 2002 by ASME

Downloaded From: https://proceedings.asmedigitalcollection.asme.org on 06/27/2019 Terms of Use: http://www.asme.org/about-asme/terms-of-use

## FATIGUE LIFE

The API2SK Recommended Practice [13] furnish a methodology based in a *T-N* curve (tension *x* number of cycles) that is normally used to predict the fatigue life of mooring line components. This methodology is exclusively based on the load applied to the component and does not consider the stress state of the component promoted by the applied load. To permit a direct comparison of the results obtained in the last section, the *S-N* method (with the modified Goodman diagram to consider the mean stress component) was used to estimate the fatigue life of the chain links [14].

In this work a stress ratio $R = 0.8$ was adopted, where $R$ is the ratio between the minimum stress ($\sigma_{min}$) and maximum stress ($\sigma_{max}$). Alternate stress ($\sigma_a$) is defined as half difference between maximum and minimum stresses, in this case is equal to $0.1 \cdot \sigma_{max}$ and mean stress ($\sigma_m$) is defined as the average value between maximum and minimum stresses and equal $0.9 \cdot \sigma_{max}$. It was assumed that the fatigue life depends on the maximum value of the *von Mises* equivalent stress.

Table 1 presents the maximum values for the *von Mises* equivalent stress for the operational load. These values were obtained from Figure 11. Regions near the load application (a 45° region from the *z* axis for paths *a* and *b*; see Fig. 1 and Fig.7) were not considered. The border of this region is indicated in Figures 11 and 12 by a vertical blue line.

Figure 13 presents a graphical insight of the predicted life for the studied cases. The four cases presented in Table 1 and 2 are place on the load line.

**Table 1 - Maximum *von Mises* equivalent stress for the operational load.**

| CASE | $\sigma_{eq}^{max}$ (MPa) | $\sigma_m$ (MPa) | $\sigma_a$ (MPa) |
|---|---|---|---|
| Elastoplastic - Studless | 570 (*d*, 0°)* | 513 | 57 |
| Elastoplastic – Stud | 381 (*e*, 21°)* | 343 | 38 |
| Elastic – Studless | 437 (*e*, 90°)* | 393 | 44 |
| Elastic – Stud | 463 (*a*, 21°)* | 417 | 46 |

* Maximum localization (path, angle measured from section A).

The endurance limit ($S_e$) was obtained considering the following conditions: surface factor in a salty corrosive environment, axial loading and ambient temperature. The predicted life (in cycles), for the four cases studied, is presented in Table 2.

**Table 2 – Predicted Fatigue Life.**

| CASE | N (number of cycles) |
|---|---|
| Elastoplastic - Studless | 30,700 |
| Elastoplastic – Stud | 768,000 |
| Elastic – Studless | 312,000 |
| Elastic – Stud | 204,000 |

It is interesting to note that the elastic models present a similar behavior (similar predicted life, but distinct critical regions): the predicted life of the studless chain link was 1,5 higher than for the stud chain link. However, the elastoplastic models present a very distinct behavior: the predicted life for the studless chain link was 25 times lower than for the stud chain link.

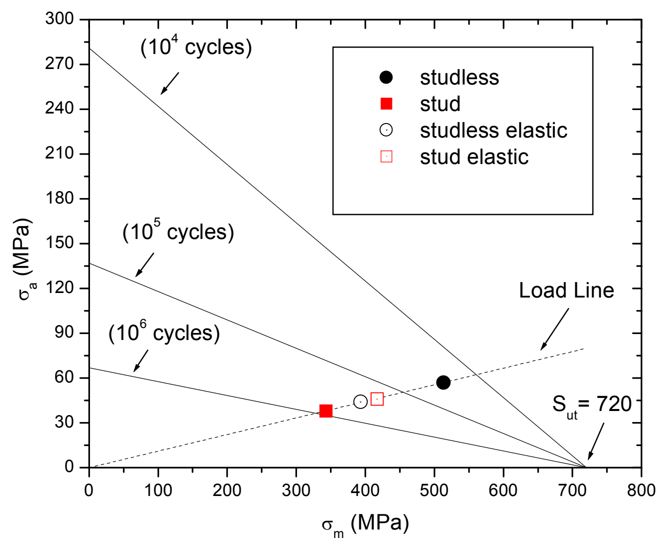


**Figure 13 – Constant life fatigue diagram**

## CONCLUSION

This work presents a study on the effect of residual stresses in the structural integrity of studless and stud chain links. A tri-dimensional finite element elastoplastic model was developed in order to determine the residual stress distribution for 92 mm studless and stud chain links.

Numerical simulation developed show that high values of residual stresses (higher than the initial yield strength) are present before the chain link enter in operation.

For a typical operational loading condition, numerical simulations show that the elastoplastic analysis furnishes a completely different stress distribution than the one obtained in an elastic analysis, due to the high level of residual stresses present in a chain link. These results suggest that an elastic


Copyright © 2002 by ASME

Downloaded From: https://proceedings.asmedigitalcollection.asme.org on 06/27/2019 Terms of Use: http://www.asme.org/about-asme/terms-of-use

analysis of the chain links is not sufficient to support a reliable fatigue analysis of this type of mechanical component.

A simplified *S-N* method was used to estimate the fatigue life of the chain links in a comparative study using the results obtained in the numerical simulations. The results show a similar predicted life for the elastic models developed for studless and stud chain links. However, the elastoplastic models present a very distinct behavior: the predicted life for the studless chain link was 25 times lower than for the stud link.

Its worth to mention that this work is an initial study on the subject and important effects as the contact phenomena that occurs between two chain links must be addresses in future works. Also a experimental program to measure residual and operational stresses must be established.

## REFERENCES


[1] Chaplin, C.R., Rebel G., and Ridge, I.M.L., 2000, "Tension/Torsion Interactions in Multicomponent Mooring Lines", *Proceedings of the 2000 Offshore Technology Conference – OTC2000*, paper OTC 12173.

[2] Papazoglou, V.J., Katsaounis, G.M., and Papaioannou, J.D., 1991, "Elastic Analysis of Chain Links in Tension and Bending", *Proceedings of the First International Offshore and Polar Engineering Conference*, Edinburgh, U.K., Vol. II, pp. 252-258.

[3] Paiva, A.M.C., 2000, "*Mooring Systems Integrity: Contributions to Metodology Analysis*" (in Portuguese), Master Degree Thesis, Department of Mechanical Engineering CEFET/RJ.

[4] API – American Petroleum Institute, 1995, "*Recommended Pratice for Design and Analysis of Stationkeeping Systems for Floating Structures*", API Recommended Practice 2SK.

[5] Hasson, D.F., and Crowe, C.R., 1988, "*Materials for Marine Systems and Structures*", Treatise on Materials Science and Technology, Vol.28, Academic Press.

[6] Stern, I.L., and Weatcroft, M.F., 1978, "Towards Improving the Reliability of Anchor Chain and Accessories", *Proceedings of the 1978 Offshore Technology Conference – OTC1978*, paper OTC 3206.

[7] SAE, 1988, *"Fatigue Design Handbook"*, SAE – Society of Automotive Engineers.

[8] Almer, J.D., Cohen, J.B. and Moran, B., 2000, "The Effects of Residual Macrostresses and Microstresses on fatigue Crack Initiation", *Materials Science and Engineering*, **A284,** pp. 268–279.

[9] Webster, G.A. and Ezeilo, A.N., 2001, "Residual Stress Distributions and their Influence on Fatigue Lifetimes", *International Journal of Fatigue*, **23,** pp. S375–S383.

[10] Ansys, 2001, "Ansys Manual", Release 5.7, Ansys Inc.

[11] ISO, 1991, "*ISO 1704 - Shipbuilding stud-link anchor chains*", 2nd Edition, International Organization for Standardization.

[12] API, 1988, *"Specification for Mooring Chain",* American Petroleum Institute Specification 2F, 5th edition.

[13] API – American Petroleum Institute, 1995, "*Recommended Practice for Design and Analysis of Stationkeeping Systems for Floating Structures*", API Recommended Practice 2SK.

[14] Shigley, J.E. and Mischke, C.R., 1989, *"Mechanical Engineering Design"*, 5th edition, McGraw-Hill.



Copyright © 2002 by ASME

Downloaded From: https://proceedings.asmedigitalcollection.asme.org on 06/27/2019 Terms of Use: http://www.asme.org/about-asme/terms-of-use